Project Title: "Determining the Impact of Forest Mortality in Semi-Arid Woodlands on Local and Regional Carbon Dynamics"
Register#: ER65412
SC#: DE-SC0008088
Final report

We received funds in July 2012, and with supplemental funds, this funding ended in July 2017. Our overall project goals were to quantify the consequences of pinon mortality for carbon, water and energy exchange in pinon-juniper woodlands. To do this, we have been continuously measuring carbon, water and energy exchange using eddy covariance, over two pinon-juniper woodlands in central New Mexico. In one site, we girdled 1632 trees in the 4 ha surrounding the tower in Sept 2009. The other site, only 5 km away on the same plateau, was left intact, to serve as a control. We used this paired tower approach so we could directly evaluate the differences between how fluxes from disturbed and intact woodlands respond to the exact same climate conditions. In addition to eddy covariance measured fluxes from the two woodlands, we also made sap flux measurements, biomass, gas exchange, and soil respiration fluxes simultaneously in the two sites. **The overall objective of this proposal is to measure the carbon and climate forcing consequences of widespread coniferous mortality events in the Southwestern US. We will incorporate these findings into a land surface model to understand the long term carbon dynamics of these mortality events and use remote sensing maps of mortality in *PJ* woodlands in NM to scale the implications of these events to regional carbon dynamics and atmospheric CO_2.** In 2013, our control PJ woodland experienced a natural pinon mortality event as bark beetles invaded the area. We received supplemental funds to quantify the extent of the mortality and how it progresses, and to add remotely sensed imagery to aid in this and estimate the loss of biomass at the site due to mortality. Finally, we have been exploring the use of both CLM and SIPNET to analyze how well these models to in representing how these woodlands change following pinon mortality. **Here, I present the results of what we have learned in these areas:**

1) how carbon, water and energy fluxes, have responded to piñon mortality, both experimentally induced and natural.
2) how we have used both ecological and remotely sensed data to quantify how the structural components of the ecosystem have changed over time following girding, and changed following natural mortality in the control site.
3) how microbial enzyme activity and decomposition rates have changed following mortality
4) how the remaining trees responded to the pinon mortality, based on sap flux data, vulnerability curves and gas exchange data; and if the disturbed woodland was more or less sensitive to climate fluctuations than the intact woodland.
5) how well the models did in representing these mortality events.

Carbon water and energy fluxes

1. A. We used an existing tower set up by Litvak in 2008 in a pinon-juniper woodland outside of Mountainair, NM for the control tower in this experiment. We set up a new tower in a pinon-juniper woodland less than 3 km away from the control site in January 2009, and girdled ~1600 pinon trees (all > 7 cm dbh) in the 4 ha footprint of the tower in

September 2009 (Figures 1 and 2). The treatment was very effective, resulting in mortality in 6 months, and most of the needles falling to the ground by August 2010 (Figure 3). Measurements of carbon, water, energy fluxes and meteorological variables at both tower sites have continued uninterrupted since 2009 (Figure 4).

B. Since the girdling, we have seen a steady decrease in carbon sequestration in response to piñon mortality which is not surprising given the 30% decrease in LAI we imposed through girdling. The sites were well matched prior to girdling. Over the 9 years since girdling was imposed, the girdled site has stored a total of ~30% less carbon than the control site (Figure 5). When we girdled, we took out only the large piñon (>7 cm dbh), and left the juniper and small piñon intact. Interestingly, carbon sequestration in the girdled site for many years was very similar to what is being measured in a nearby juniper savanna. In all years, except 2013, the juniper savanna site sequestered more carbon than the disturbed site (Fig. 5-6).
C. Cumulative gross primary productivity and respiration from 2009-2016 were both ~30% lower in the girdled site relative to the control site (Figure 5). Relative to the control site, both the girdled site and juniper site had lower GPP and RE until 2013, when natural mortality was first observed in the control site. After 2013, the differences between these sites and the control site decreased. We have been somewhat surprised that we have seen no obvious increase in respiration relative to gross primary productivity suggesting that decomposition of the dead organic material from the girdled trees has not increased dramatically in the time period we have been making our measurements. We have only seen brief periods where the ratio of respiration to gross primary productivity was higher in the girdled site, and this does not appear to be related to precipitation. Litter respiration in these sites is limited more by water than substrate though, as was pointed out in Berryman et al. (2013) (Figure 7). Andy Fox is almost ready to submit a paper on the carbon balance consequences of girdling.

D. We have seen no significant change in either sensible heat or latent heat fluxes due to the pinon mortality we imposed, or to the natural mortality event at the control site in 2013. (Figures 8 and 9). This was somewhat surprising, but we concluded that LAI and canopy density was so low, that extra mortality did not alter ecosystem sufficiently to trigger ecosystem scale changes in the energy balance. We discussed the water balance component changes in Morillas et al. 2017. Cheng-Wei Huang is currently preparing a manuscript discussing the surprising lack of energy balance changes we have observed at the site and tying it to other disturbances in semi-arid biomes.

2. Structural changes in response to both girdling and natural mortality:

A. We collaborated with Lee Vierling and Jan Eitel from University of Idaho to use RapidEye remotely sensed data products to determine how long it took for RapidEye, MODIS and Landsat products to detect the first signs of chlorosis and mortality following the girdling. This is all detailed in Eitel et al. 2011.
B. Dan Krofcheck's dissertation (PhD student in Litvak's lab), synthesized remotely sensed data of the intact and disturbed PJ woodlands. His paper to Remote Sensing of the Environment (Krofcheck et al. *2014*) relating the structural changes we detected remotely to functional changes measured with the eddy covariance towers. The highlights of this research were 1) using crown-level remotely sensed time series from RapidEye to track changes in a PJ woodland following disturbance; 2) detecting and relating changing in canopy LAI to tower-based measure of productivity; 3) detecting changes in herbaceous understory and relating these changes to the degree of coupling between tower-based GPP and reflectance indices. Greenness indices in our disturbed woodland were much more sensitive to changes in soil water content compared to this relationship in the intact PJ woodland, reflecting the greater contribution of the understory to structure. The changes in the understory have not contributed substantially to changes we have measured at the tower scale.
C. Krofcheck's second manuscript (Krofcheck et al. 2015) used remotely sensed driven linear models to estimate GPP in both intact and disturbed PJ woodlands. He originally tested how much the model is improved by using MODIS vs. RapidEye data, and whether or not canopy water content from MODIS varies enough to sufficiently represent how sensitive productivity in these ecosystems is driven by soil water availability. Given the small size of the PJ girdled plot, we were concerned that MODIS pixel was too large to adequately reflect only the girdled site, so he downloaded the complete Landsat dataset for this region and redid the whole analysis using data from 30 m pixels. The fits are much stronger now and the conclusions will be too. This should be submitted in the next two weeks.
D. We also have airborne Lidar data acquired in summer of 2011 over both the disturbed and intact PJ woodlands processed and are coupling this to data from Worldview-2 images acquired at the same time over both of these sites. Combining these two datasets has helped tremendously in vegetation classification. Dan's third mansucript from his thesis (Krofcheck et al. 2016) used Lidar data to estimate juniper biomass and validated it with ground measurements. This is tricky because juniper is not a single stem, easy to measure tree. They have come up with a plan to use our ground data to be able to estimate juniper biomass on large spatial scales.
E. We are currently developing a sUAS derived, scalable allometric assessment of carbon stocks in pinon-juniper woodlands. We have developed a scalable and robust biomass estimation framework using the repeat structure from motion (SfM) imagery collected at the two flux tower sites on the Deer Canyon Plateau. SfM workflows are often associated with large geometric uncertainties, resulting in appreciable scaling

errors, especially when applied in natural systems. Our SfM approach focuses heavily on the characterization and propagation of uncertainty from the initial image acquisition, through processing and geolocation, to the creation of species specific allometric relationships using existing, peer-reviewed data. Our workflow is simple, extensible, and affords the integration of various existing earth observation (EO) passive optical satellite platforms such as the Landsat and Sentinel constellations. By combining SfM and EO data sets, we have a built a framework that will allow the direct spatial scaling of empirical relationships between the changes in structural vegetation due to drought or pest outbreak and site-specific observations of ecosystem function from in-situ measures of carbon, water, and energy exchange.

F. Currently, we have completed the creation of remotely driven allometric equations for pinon and juniper, capable of explaining greater than 73% of the variation in whole tree biomass using remotely sensed tree characteristics alone (namely volume and maximum height) (Figure 10). This approach requires the description of the study area be split into individual canopy objects or tree crowns, which in turn affords a broad variety of modeling opportunities. We intend to use these data to drive the foundation of an eddy-covariance – satellite EO linked model of ecosystem function, wherein we contextualize the tower fluxes using changes in the reflectance data on a per-crown basis. Specifically, we are moving forward with using multi-temporal passive optical EO satellite data to model the foliar reflectance of individual canopy objects to scale carbon, water, and energy balance across the fetch of the eddy covariance towers. An initial publication describing the application of the SfM derived allometric scaling of whole tree and foliar biomass (in both live and dead carbon pools) as characterized during a severe drought event is being finalized and will be submitted by June 1, 2018 (Figure 11). The broader application of the SfM, EO, and eddy-covariance data sets will be used to continue to monitor carbon stocks as a function of climatic and biotic stress throughout the measurement record of the flux tower network.

G. We first observed the piñon mortality on the plateau where both the girdled and control towers are located in 2013 (Figure 12). Because of this we started doing dead tree surveys annually in the 4 ha plot surrounding our tower, where we recorded the GPS location of every dead tree, species, height, dbh, and whether or not it had evidence of bark beetle activity (Figures 13, 14). This allowed us to quantify the extent and progress of this natural mortality event and in particular, quantify the decrease in sapwood area of each species (Figure 15).

H. Interestingly, a sapling survey we just did in March 2018 indicates greater pinon regeneration in the control plot than the girdled plot (Figure 16). This has really interesting implications for how these disturbed woodlands are going to change following these large scale mortality events. We suspect that because 2009/2010

winter was so wet, there was a large germination event in 2010, a year following the girdling in the girdled site.

I. We have also been collaborating with Chris and Cait Lippit, professors in the Geography department at University of New Mexico to use Landsat to quantify quantifying differential piñon and juniper mortality by performing multiple endmember spectral mixture analysis on six Landsat images from 2009 through 2015 using field-based spectra collected throughout 2015. An ideal spectral separability time of year was identified to maximize separation between constituent land-cover classes by calculating vegetation indices for the five dominant land-cover classes at the site (juniper, piñon, dead piñon, herbaceous, and soil). Ideal separability periods were also determined by evaluating precipitation and temperature data. Peak separabililty between land-cover classes within the study period was determined to occur during the pre-monsoon season between late spring/early summer (May) when minimal spectral overlap occurred between classes ($\sigma = 1$). The fieldbased spectra were then used to unmix each image in the study period. Results indicate a 24.6% decline of piñon across the study period with a comparable 23.8% increase of dead piñon. Accuracy assessment using high spatial (5–8 cm) resolution imagery for 2014 and 2015 showed strong correlation with modelled fractional cover results for 2014: live piñon and juniper ($R2 = 0.72$), and dead piñon ($R2 = 0.79$), and 2015: live piñon and juniper ($R2 = 0.77$), dead piñon ($R2 = 0.65$). Results demonstrate the potential of MESMA to monitor and accurately quantify the differential dieoff of piñon and juniper at a regional scale as climate changeinduced drought and higher temperatures are projected to continue in the Southwest. This is from Brewer et al. 2017.

3. Microbial enzyme activity and decomposition rates have changed following mortality

A. To assess the effects of this large scale mortality on soil processes, we analyzed rhizosphere extracellular enzyme activity (EEA) and fungal biomass in soil samples collected beneath tree canopies at two PJ woodland sites: one site where pinons were experimentally killed by girdling, and a paired intact site with no piñon mortality that served as a reference. We also quantified soil water content (SWC) from soil samples, and sap flow density fluxes as an indicator of tree physiological status. Soil EEA patterns varied as functions of the identity of the closest competitor trees, host-tree physiological status, and SWC. At the girdled site, we observed higher plant cell wall related decomposition activities under live juniper canopies, compared to dead piñon trees. In contrast, at the control site, we observed higher plant cell wall decomposition rates under live pinon rather than juniper canopies, particularly with higher soil moisture availability. At the site level, ordination plots for intact PJ woodlands showed a decreasing trend in microbial cell wall decomposition activity as soil water availability, and fungal biomass increased. We observed the opposite trend at the girdled site. Overall, these results suggest that widespread pinon mortality significantly affects the functional

behavior of rhizosphere microorganisms at multiple scales, in part by shifting the focal substrates of microbial community decomposition. This was all detailed in Warnock et al. 2016.

4. Response of the remaining trees to pinon mortality, based on sap flux data, vulnerability curves and gas exchange data

A. Amanda Liebricht, a graduate student of Litvak who is defending this month looked for evidence of competitive release in the remaining trees following the girdling. She found no evidence of this in gas exchange data, vulnerability data, or biomass data (Fig 17, 18, 19). Amanda defends her PhD dissertation in two weeks and this is first chapter that will be submitted in summer 2018.

B. Laura Morillas, a postdoc with Litvak, examined the sap flow rates in the remaining pinon and juniper in the girdled and compared them to the sap flow rates of these species in the control plot and found that, consistent with Amanda's work, there was no evidence of competitive release in these species. In fact sap flow rates in the girdled plots were lower than in the control sites (Figure 20). This was in Morillas et al. 2017.

C. In fact, it appears that girdling altered the partitioning of ET such that the contribution of canopy transpiration to ET decreased 9-14% over the study period, relative to the intact control, while non-canopy ET increased. We attributed the elevated non-canopy ET in the girdled site each year to winter increases in sublimation, and summer increases in both soil evaporation and below-canopy transpiration. Although we expected that mortality of a canopy dominant would increase the availability of water and other resources to surviving vegetation, we observed a decrease in both soil volumetric water content and sap flow rates in the remaining trees at the girdled site, relative to the control. This post-girdling decrease in the performance of the remaining trees occurred during the severe 2011-2012 drought, suggesting that piñon mortality may trigger feedback mechanisms that leave PJ woodlands drier relative to undisturbed sites, and potentially more vulnerable to drought. This is all detailed in Morillas et al. 2017. Interestingly, the decrease in soil water availability we observed at the girdled site following the girdling, is now reversing after the natural mortality event in the control site (Figure 21).

D. The disturbed woodland also appears to be more sensitive to climate fluctuations than the intact woodland (Figure 6). The girdled site converted from a carbon sink to a carbon source in 2013 following 2 ½ years of drought, while the control site remained a sink. Interestingly, the control site started to experience in mortality in 2013.

5. ***Modeling activities***

A. Modeling the manipulation experiment with the Community Land Model 4.5. Using Community Land Model version 4.5-Biogeochemisty (BGC) in PTCLM mode we spun up an 80-member model ensemble for 2000 years cycling through 12 years of available climate drivers that were available for the site location from an 80-member ensemble of the Community Atmosphere Model. This provides uncertainty in the climate experienced at this location, and results in a spread of initial conditions in the modeled ecosystem states on 1 January 2009, when we then switched to local site meteorology to drive the model forward for 3 years. Starting on 1 October 2009 we manipulated the model restart files to move 8% of live carbon and nitrogen pools to dead pools each month for 6 months, which resulted in a total reduction of then C and N pools by 40% (Fig. 22). Over this time period the model simulated latent heat flux well (Fig. 23). Observations indicated the manipulation reduced LE by 6.9% during this period, whilst the model simulated a 5% reduction. However, it does seem that the impact of the manipulation persists more strongly into the second year post-disturbance in the observed fluxes, whilst the impact is nearly completely muted in the model by this time.

Using sapflow measurements we were able to partition evapotranspiration flux in to transpiration and soil evaporation and compare this to the model. CLM suggests this change in vegetation results in a reduction of transpiration of 49%, whilst observations show only a 17% reduction, with corresponding increases in soil evaporation of 19% and 16% respectively (Fig. 24). Observations of soil moisture at the manipulation site suggested that whilst ET was reduced as expected, soil moisture was also reduced by 6%. This is counter to expectation, and this is highlighted by the model that ensures a water balance within the confines of the represented processes. Consequently the modeled reduction in ET causes a 5% increase in soil moisture (Fig. 25). Whilst the performance of the model in simulating LE is impressive at this semi-arid location, unfortunately CLM is known to simulate carbon fluxes poorly in such environments. We see this in very different ecosystem water use efficiencies between the observations and in the model (Fig. 26).

This bias in CLM4.5 for simulating productivity in semi-arid areas is likely to be due to a combination errors in different parts of the model, including plant hydraulics and treatment of dry season phenology and C4 grasslands. Addressing these were beyond the scope of this project, so we did not attempt detailed analysis of carbon dynamics at the site level using this version of the model (although some of these errors have now been addressed by other developers within CLM5.0, released in February 2018). However, we have been able to continue the develop data assimilation capability with CLM using the Data Assimilation Research Testbed (DART) that we proposed using to do this analysis in a more holistic way.

B. Data assimilation with CLM-DART using large-scale remote sensing observations

In work shortly to be submitted to the open-access AGU journal Journal of Advances in Modeling Earth Systems we demonstrate that our system can assimilate 10 years of satellite-derived monthly leaf area index and annual biomass observations over a 0.25 degree area of New Mexico, centered on the control site location. Again, we found that the prior model did not compare favorably with the observations for this semi-arid site, with systematic bias in magnitude of both LAI and biomass and an apparent failure to correctly represent the phenology and environmental sensitivity of LAI (Fig. 27). For the purposes to this work that focused on the technical development of the DA system, we treated the observations, and their associated uncertainties as being accurate, and ascribe the model-data mismatch to being a function of model error. That is to say, we have more confidence in the observations than in the model at this location, and do not attempt any bias correction on the observations. We asked whether the EAKF can overcome these large data-model mismatches.

We find that the EAKF can overcome the large bias and apparent model error if we implement a technique to inflate the forecast error variance, which we define as the spread of the ensemble. In experiments where we limited the allowable mismatch to 3 standard deviations we found that only the highest LAI values were included in the assimilations (Fig. 28a, top panel) and that all the biomass values were ignored (Fig. 28b top panel). In contrast, by implementing adaptive inflation routines within DART, the model error is increased in response to the relative model-data mismatch. There is large reduction in the root mean square error (RMSE) in LAI and biomass for the adaptive inflation experiment (red curve), both relative to the free-run (black curve) and no-adaptive inflation experiment (green curves in Fig. 28e and 28f bottom panels). For LAI RMSE over the 10 year period of the assimilation is reduced by over 50%, from 0.93 m^2 m^{-2} to 0.44 m^2 m^{-2} and by 70% for biomass from 1376 gC m^{-2} to 418 gC m^{-2} (Table 1). The success of the EAKF illustrates a clear application to solve biases in initial conditions resulting from incorrect model spin-up. In this example, we are explicitly trusting the data more than the model, however we see great potential for diagnostic studies; we can use the ENKF to ensure that the model will estimate carbon, water and energy budgets which are consistent with available data. This could help constrain changes in the historical global land carbon budget due to land use and land cover change processes not yet robustly implemented in models given the wealth of global satellite observations and other LSM benchmarks over the last several decades.

C. Simulating site level carbon dynamics with an ecosystem model Because we found that CLM simulated the site level carbon dynamics poorly at our site we switched to an ecosystem model that could be more easily parameterized at this specific location using eddy covariance flux observations. This work is shortly to be submitted to AGU Journal of Geophysical Research – Biogeosciences. The purpose of our modeling exercise was to generate a model simulation of C fluxes that is well-calibrated to the pre-treatment behavior of the ecosystem, such that it may be temporally extrapolated to provide estimates of hypothesized C fluxes after the treatment. For this process we used the SIPNET model, in conjunction with a Markov chain Monte-Carlo (MCMC) parameter estimation methodology. SIPNET simulates the carbon dynamics between the atmosphere, vegetation pools, leaves and wood (combined bole, branches) and roots, and a single soil pool on twice daily time steps: day and night. GPP is simulated using an initial, unstressed rate, that is reduced as a function of four scaling factors controlled by: (i) air temperature; (ii) vapor pressure deficit (VPD); (iii) available photosynthetically active radiation (PAR); and (iv) moisture stress. Respiration from the leaf and wood carbon pools is modeled as a Q10 function of air temperature and pool size. Soil respiration is similarly modeled as Q10 function, but uses soil temperatures and is reduced in proportion to fractional soil wetness when soil temperatures are above zero. We used a variation of the Metropolis algorithm to estimate 17 of 32 model parameters and the initial conditions. Of the remaining 15 values required, initial plant wood carbon, leaf area index, soil carbon, and specific leaf area were prescribed with site measurements and the other 13 values were held at default values used at other evergreen, needle leaf sites. Following calibration 100 of the accepted parameter sets were then randomly selected and used to generate a 100-ensemble member forward run of the model which was then used to generate mean model states and fluxes and their confidence limits. Experimentation found 100-ensemble members to be the minimum required to produce stable mean and confidence limits estimates.

After parameterizing the SIPNET model using data available at the control site, we then ran the model at the manipulation site using these parameters and site-specific initial conditions and meteorological drivers to estimate the carbon fluxes from this site if the manipulation hadn't occurred. The optimized model at the control site over estimates C uptake in the early part of the record (Figure 29 and Table 2) although it is more satisfactory from summer 2010 onwards. During the post-treatment period SIPNET estimates c.15% greater C uptake. In contrast, at the manipulation site prior to treatment when direct comparisons are possible, SIPNET underestimates C uptake by c. 20% (Table 2). Post-treatment, SIPNET estimates of NEE at the manipulation site (when girdling is *not* simulated) are in relative agreement with the normalized control values and total C uptake post-treatment overlap within our confidence limits (-572 +-19 gC m^{-2} compared to 548 +-30 gC m^{-2}, Table 2). The close agreement between these modeled results, and flux observations corrected for pre-treatment inter-site differences gives us

confidence that our estimate of the treatment effect using this process-based modeling approach of 311 gC m^{-2}, a 54% reduction over this two year period.

Products:

Truettner, C., W.R.L. Anderegg, F. Biondi, G.W. Koch, K. Ogle, C. Schwalm, M.E. Litvak, J.D. Shaw and E. Ziaco. Conifer Radial Growth Response to Recent Seasonal Warming and Drought from the Southwestern USA. In press, Forest Ecology and Management.

Morillas, L., R.E. Pangle, G.E. Maurer, W.T. Pockman, N. McDowell, C-W. Huang, D.J. Krofcheck, A.M. Fox, R.L. Sinsabaugh, T.A. Rahn, M.E. Litvak. 2017. Tree mortality decreases water availability and ecosystem resilience to drought in pinon-juniper woodlands in the southwestern USA. JGR-Biogeosciences 122, 3343–3361. https://doi.org/ 10.1002/2017JG004095JGR-Biogeosciences

Brewer, W., C. Lippit, M.E. Litvak, C. Lippit. Assessing drought-induced change in a pinon-juniper woodland with Landsat: a multiple endmember spectral mixture analysis approach. International Journal of Remote Sensing. 38:14, 4156-4176, DOI: 10.1080/01431161.2017.1317940

Villegas, J. C., D. J. Law, S. C. Stark, D. M. Minor, D. D. Breshears, S. R. Saleska, A. L. S. Swann, E. S. Garcia, E. M. Bella, J. M. Morton, N. S. Cobb, G. A. Barron-Gafford, M. E. Litvak, and T. E. Kolb. 2017. Prototype campaign assessment of disturbance-induced tree loss effects on surface properties for atmospheric modeling. Ecosphere 8(3):e01698. 10.1002/ecs2.1698

Krofcheck, D.J., M.E. Litvak, C.D. Lippitt, and A. Neuenschwander. 2016. Woody biomass estimation in a Southwestern US juniper savanna using clumped tree segmentation and existing allometries. Remote Sens. 2016, 8(6), 453; doi:10.3390/rs8060453

Wolf, S., T.F. Keenan, J.B. Fisher, D.D. Baldocchi, A.R. Desai, A.D. Richardson, R.L. Scott, B.E. Law, M.E. Litvak, N.A. Brunsell, W. Peters, I.T. van der Laan-Lujikx. 2016 Warm spring reduced carbon cycle impact of the 2012 US summer drought. PNAS 113(21), 5880–5885, doi: 10.1073/pnas.1519620113.

Biederman, J. A., Scott, R. L., Goulden, M. L., Vargas, R., Litvak, M. E., Kolb, T. E., Yepez, E. A., Oechel, W. C., Blanken, P. D., Bell, T. W., Garatuza-Payan, J., Maurer, G. E., Dore, S. and S. P. Burns. 2016. Terrestrial carbon balance in a drier world: the effects of water availability in southwestern North America. Global Change Biology doi:10.1111/gcb.13222.

Stark, S.C., D.D. Breshears, E.S. Garcia, D.J. Law, D.M. Minor, S.R. Saleska, A.L.S. Swann, J. C. Villegas, L. E.O. C. Arago, E. M. Bella, L.S. Borma, N.S. Cobb, M. E. Litvak, W. E. Magnusson, J.M. Morton, M.D. Redmond. 2016. Toward accounting for ecoclimate telconnections: intra- and inter-continental consequences of altered energy balance after vegetation change. Landscape Ecol. 31:181-194. DOI 10.1007/s10980-015-0282-5.

Warnock, D.D., M.E. Litvak, L. Morillas, R.L. Sinsabaugh. 2016. Drought-induced pinon

mortality alters the seasonal dynamics of microbial activity in pinon-juniper woodland. Soil Biol Biochem, 92: 91-101.

Krofcheck, D. J., J.U.H. Eitel, C.D. Lippitt, L. A. Vierling, U. Schulthess, and M. E. Litvak. 2015 Remote sensing based simple models of GPP in both disturbed and undisturbed pinon-juniper woodlands in the Southwest U.S. *Remote Sens.* **2015**, *8*(1), 20; doi:10.3390/rs8010020.

Dean, S., D. Warnock, A.P.-Alfaro, M. Litvak, and R. Sinsabaugh. 2015. Root Associated Fungal Community Response to Drought-Associated Changes in Vegetation Community. Mycology, 107(6): 1089-1104; doi: 10.3852/14-240

Cueva, A. M. Bahn, M. Litvak, J. Pumpanen, R. Vargars. 2015. A multisite analysis of temporal random errors in soil CO_2 efflux. JGR Biogeosciences DOI 10.1002/2014/JG002690.

McDowell, N.G., N.C. Coops, P. Bieck, J. Chambers, C. Gangodagmage, J.A. Hicke, C. Huange, R. Kennedy, D. Krofcheck, M. Litvak, A. Meddens, J. Muss, R. Negron-Juarez, C. Peng, A. Schwantes, J. J. Swenson, L. Vernon, A. P. Williams, C. Xu, M. Zhao, S. Running and C. Allen. 2014. Global satellite monitoring of climate-induced vegetation disturbances. Trends in Plant Science. *20 (2), 114-123.*

Krofcheck, D.J., J. U.H. Eitel, L.A. Vierling, U. Schulthess, E. Dettweiler-Robinson, R. Pendleton, and M.E. Litvak. 2014. Linking structural with functional changes in a piñon-juniper woodland using a time series of high spatial resolution satellite data and eddy covariance. Remote Sensing of the Environment, Remote Sensing of Environment 151, 102-113; http://dx.doi.org/10.1016/j.rse.2013.11.009.

Meyer, N.A., D.O. Breecker, M.H. Young, M.E. Litvak. 2014. Simulating the role of vegetation in formation of pedogenic carbonate. Soil Science Society of America Journal 78 (3), 914-924, doi:10.2136/sssaj2013.08.0326.

Berryman, E., J.D. Marshall, T. Rahn, M.E. Litvak and J. Butnor. 2013. Decreased carbon limitation of litter respiration in a mortality-affected piñon-juniper woodland. Biogeosciences, 10: 1625-1634.

Eitel, J.U.H., L. A. Vierling, M.E. Litvak, D. Krofcheck, D.S. Long, A.A. Ager, A. Hudak and L. Stoscheck. 2011. Broadband, red-edge information from satellites improves early stress detection in conifer forests. Remote Sensing d*oi:10.1016/ j.rse.2011.09.002*

Berryman, E.M, Marshall, J.D., Rahn, T., Cook, S.P. and Litvak, M. 2011. Adaptation of continuous-flow cavity ring-down spectroscopy (CRDS) for batch analysis of $\delta^{13}C$ of CO_2. Rapid Communications in Mass Spectrometry 16:2355-60.

Eitel, J.U.H., L.A. Vierling, D.S. Long, M. Litvak, K.B. Eitel. 2011. Simple assessment of needleleaf and broadleaf chlorophyll content using a flatbed color scanner. Can J For Res 41:1445-1451.

Invited talks

Litvak, M.E. 2016. Quantifying the response and resilience of carbon dynamics in semi-arid biomes in the Southwestern US to drought. 101st ESA annual meeting, Aug 7-12, 2016. Ft. Lauderdale, FL.

Litvak, M.E. 2015. Detection of extreme climate events in semi-arid biomes using a combination of near-field and satellite based remote sensing across the New Mexico Elevation Gradient network of flux towers. AGU Fall Meeting Dec. 12-16, 2015, San Francisco, CA.

Litvak, M.E., 2015. Quantifying the resilience of carbon dynamics in semi-arid biomes in the Southwestern US to drought. 2015 AGU Fall Meeting, Dec. 12-16, 2015, San Francisco, CA.

Litvak, M.E. 2014. Carbon and energy balance consequences of widespread mortality in Piñon-Juniper Woodlands. TES/SBR Joint Investigators Meeting, May 6-7, 2014. Plenary. Potomac, MD.

Litvak, M.E., D. Krofcheck, L. Morillas, T. Hilton. A. Fox, 2014. Local to regional scale energy balance consequences of widespread mortality in piñon-juniper woodlands. 2014 AGU Fall Meeting, December 15-19, San Francisco, CA.

Litvak, M.E., D. Krofcheck, L. Morillas, A. Fox, 2014. Observing and Quantifying Ecological Disturbance Impacts on Semi-Arid Biomes in the Southwestern US. 2014 AGU Fall Meeting, December 15-19, San Francisco, CA.

Krofcheck, D. L. Morillas, M. Litvak. 2014. Investigating the biophysical controls on mass and energy cycling in Southwestern US ecosystems using the New Mexico Elevation Gradient of flux towers. 2014 AGU Fall Meeting, Dec 15-19, San Francisco, CA.

Litvak, M.E.; D. Krofcheck; Timothy W. Hilton; Andrew M. Fox. Quantifying the vulnerability of carbon stocks and fluxes in six semi-arid biomes in the Southwestern US to the severe 2011-2013 drought 2013 AGU Fall Meeting, December 9-13, San Francisco, CA.

Litvak, M.E. T. Hilton, D. Krofcheck, A. M. Fox, R. Sinsabaugh, N. McDowell, T. Rahn, A. Neuenschwander. Carbon and energy balance consequences of widespread mortality in piñon-juniper woodlands. 2013 Ecological Society of America Annual Meeting, August 4-9, Minneapolis, MN.

Litvak, M.E. Vulnerability, thresholds, tipping points: TE response to the USGCRP 2015 agenda 2013 NASA Terrestrial Ecology Science Team Meeting. Plenary. April 30-May 2, 2013. La Jolla, CA.

Litvak, M.E., T. W. Hilton, D. Krofcheck, A.M, Fox, A. Neuenschwander. 2013. Quantifying the vulnerability of carbon stocks and fluxes in six semi-arid biomes in the Southwestern US to both temperature and precipitation extremes. Plenary. 2013 Ameriflux/NACP Meeting, Feb. 4-7, 2013. Albuquerque, NM.

Contributed talks

Fox, A.M., D.J. Krofcheck, A. Liebricht, G. Maurer, L. Morillas, R. E. Pangle, W.T. Pockman, S. Schwinning and M.E. Litvak. Detecting hydrological tipping points in semi-arid woodlands. ESA Annual Meeting. Aug- 8-12, 2016. Ft. Lauderdale, FL.

Krofcheck, D., C.Lippitt, A. Loerch, M.E. Litvak. 2015. Repeat, low altitude measurements of vegetation status and biomass using manned aerial and UAS imagery in a pinon-juniper woodland. AGU 2015 Annual Meeting Dec 9-14, 2015. San Francisco, CA.

Krofcheck, D., C. Lippitt, M. Litvak. Impacts of drought on regional carbon uptake dynamics in the Southwestern US, using the New Mexico Elevation Gradient of flux towers and the Temperature-Greenness model. 2014 AGU Fall Meeting, December 15-19, San Francisco, CA.

Morillas, L. R. Pangle, D. Krofcheck, W. Pockman, M. Litvak. 2014. Consequences of Widespread Piñon Mortality for Water Availability and Water Use Dynamics in Piñon-Juniper Woodlands. 2014 AGU Fall Meeting, December 15-19, San Francisco, CA.

Warnock, D. M. Litvak, R. Sinsabaugh. 2014. Disturbance events affect interactions among four different hydrolytic enzymes in arid soils. 2014 AGU Fall Meeting, December 15-19, San Francisco, CA.

Warnock, D, M. Litvak and R. Sinsabaugh. 2014. Summer monsoon rains affect litter decomposition dynamics beneath tree canopies in a Piñon-Juniper Woodland. Nov 2-5, 2014. Long Beach, CA.

Warnock, D., M. Litvak, and R. Sinsabaugh. 2014. Piñon mortality and summer monsoon rains affect extracellular enzyme activity of soil microbial communities living beneath tree canopies in a Piñon-Juniper Woodland. 2014 Annual Meeting. Soil Science Society of America Nov 2-5, 2014. Long Beach, CA.

Morillas-Gonzales, L., D. Krofcheck, R. Lefevre, and M. Litvak 2014. Interactions between transpiration, tree mortality and canopy temperature in semiarid woodlands. 2014 ASABE (American Society of Agricultural and Biological Engineers) meeting. Evapotranspiration: Challenges in Measurement and Modeling from Leaf to the Landscape Scale and Beyond.

Krofcheck, D., A. Neuenschwander, A. Fox, M.E. Litvak. Spatial scaling of waveform lidar data within Eddy-flux tower fetch to characterize heterogeneity of semi-arid ecosystems NASA Terrestrial Ecology Science Team Meeting. April 30-May 2, 2013. La Jolla, CA.

Litvak, M.E. 2012. Use of a flux tower network to monitor and model Southwestern U.S. biome responses to climate change. Los Alamos IGPP meeting, Southwest Climate: Past, Present and Future. Sept 5-7, 2012. Jemez Springs, NM.

Warnock, D.D.; M.E. Litvak, R.L. Sinsabaugh. Piñon mortality and summer monsoon rains affect extra cellular enzyme activity of soil microbial communities living beneath tree canopies in a Piñon-Juniper woodland . 97th Annual Meeting, Ecological Society of America. Portland, OR Aug 6-10, 2012.

Graduate students trained

Daniel Krofcheck
Amanda Liebricht
Erin Berryman
Will Brewer
Zach Taraschi

Undergraduates trained

Amanda Liebricht REU
Ileana Betancourt REU
Maxine Paul REU
Elida Iniguez REU

Postdocs
Andy Fox
Laura Morillas
Dan Krofcheck

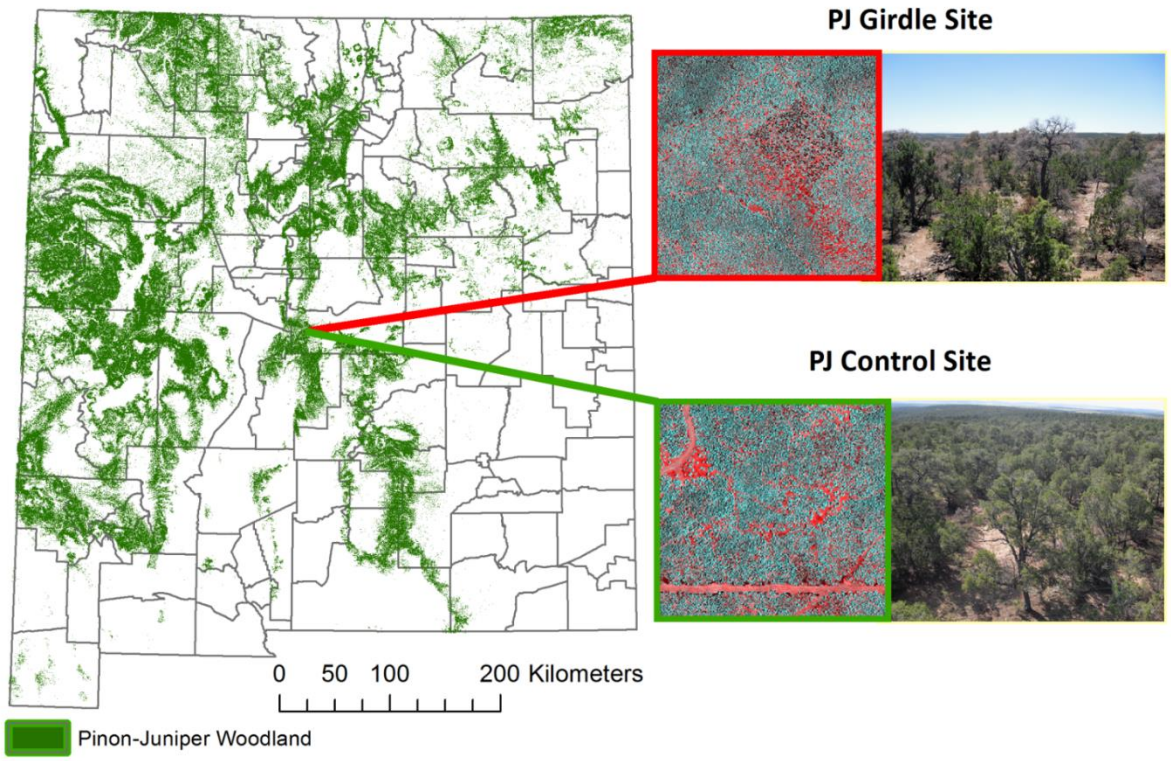

Figure 1. Piñon-juniper control and girdled sites on plateau south of Mountainair, NM.

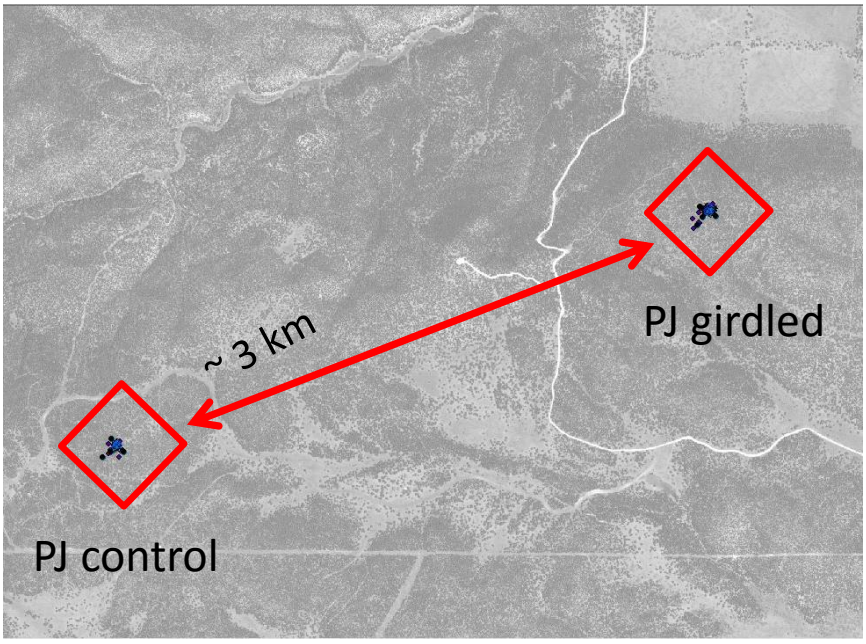

Figure 2. Paired woodlands are located only 3 km apart from each other. The entire plateau is covered by PJ woodland.

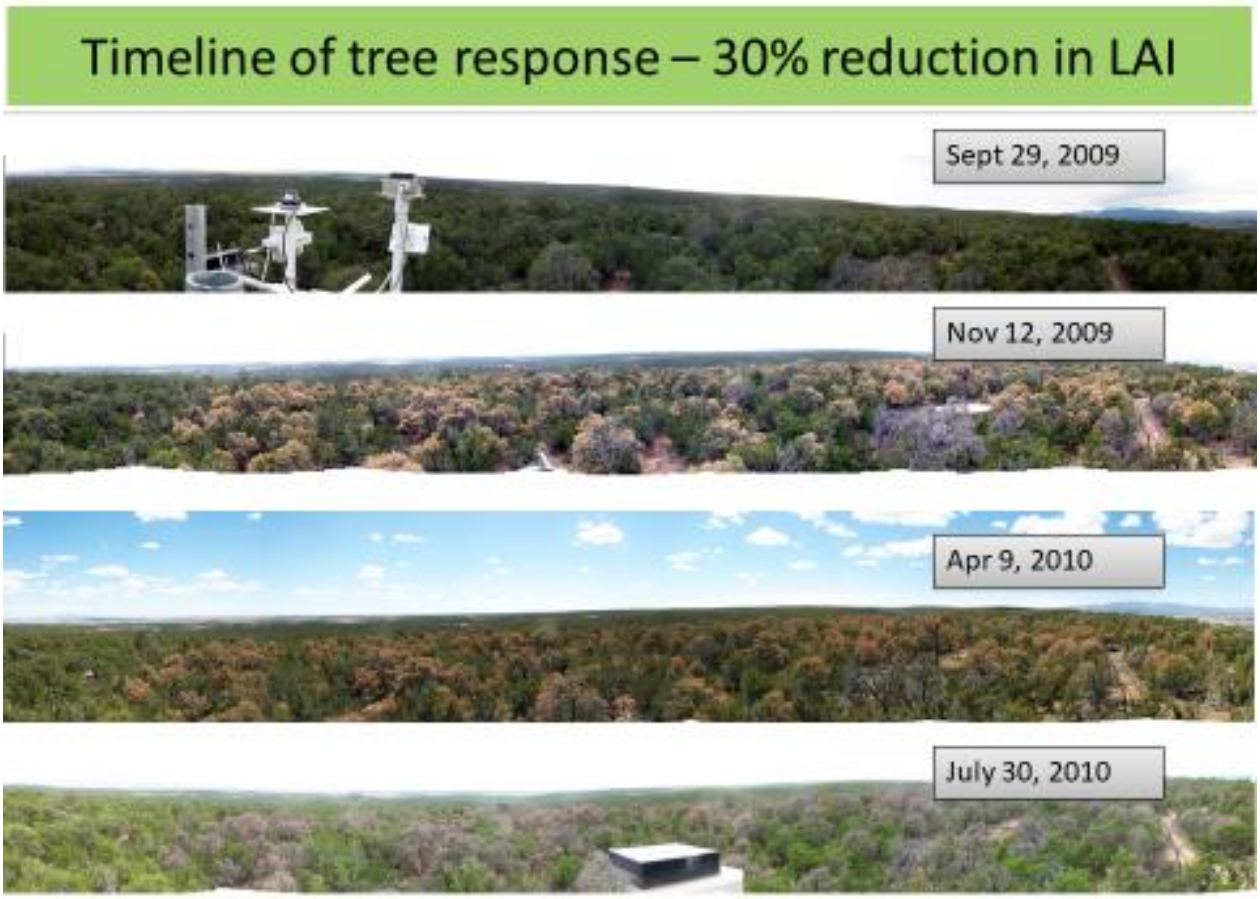

Figure 3. Timeline of the response from the girdling. The treatment of girdling the trees about 3 ft from the ground, and injecting 5% glyphosphate solution into the cut resulted in chlorosis within 2 months, obvious mortality in 6 months, and needles falling from the trees in about 10-12 months.

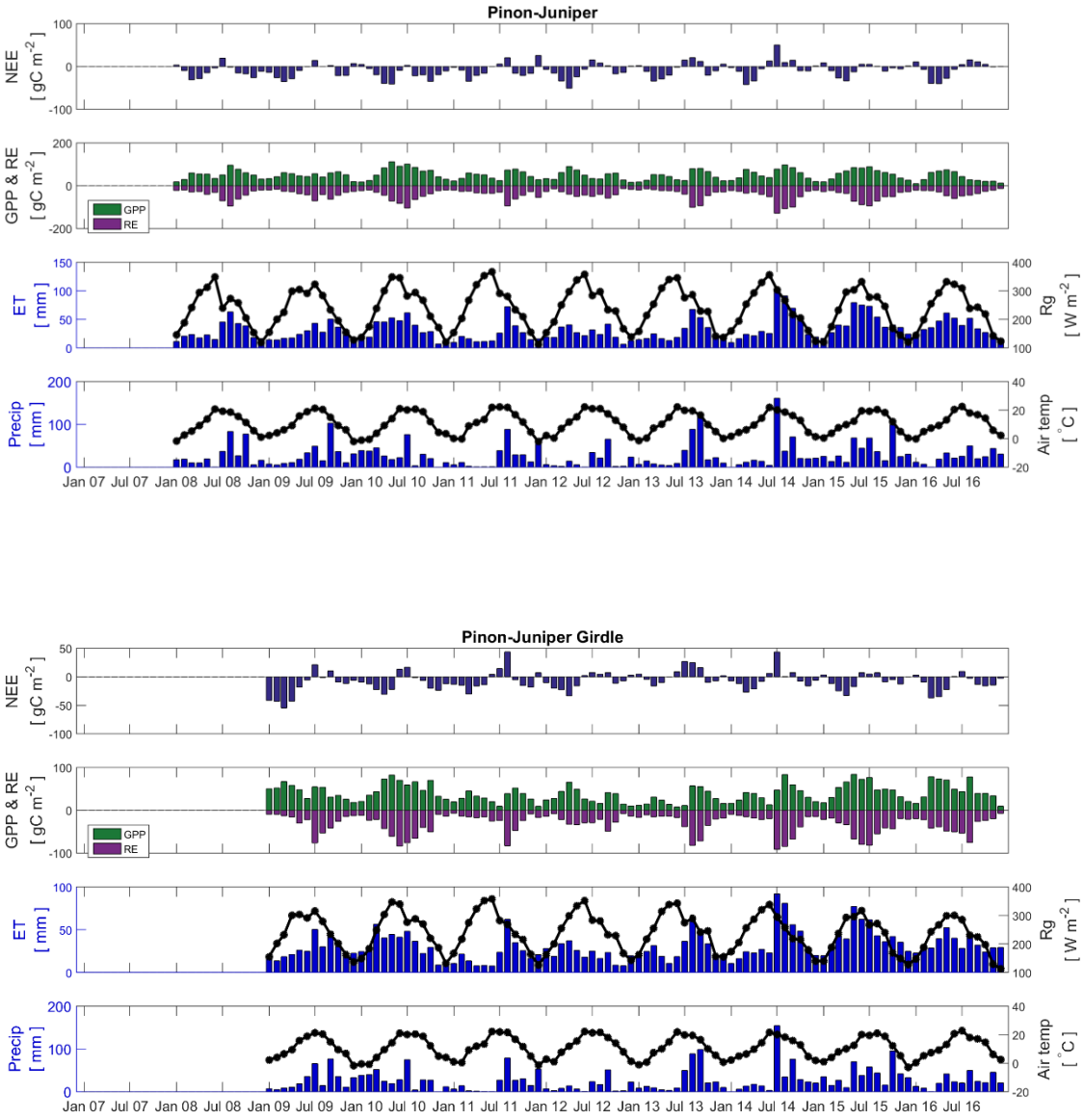

Figure 4. Monthly NEP, GPP, Re, ET, Mean temperature, Total Precipitation at PJ control and PJ Girdle 2009-2016.

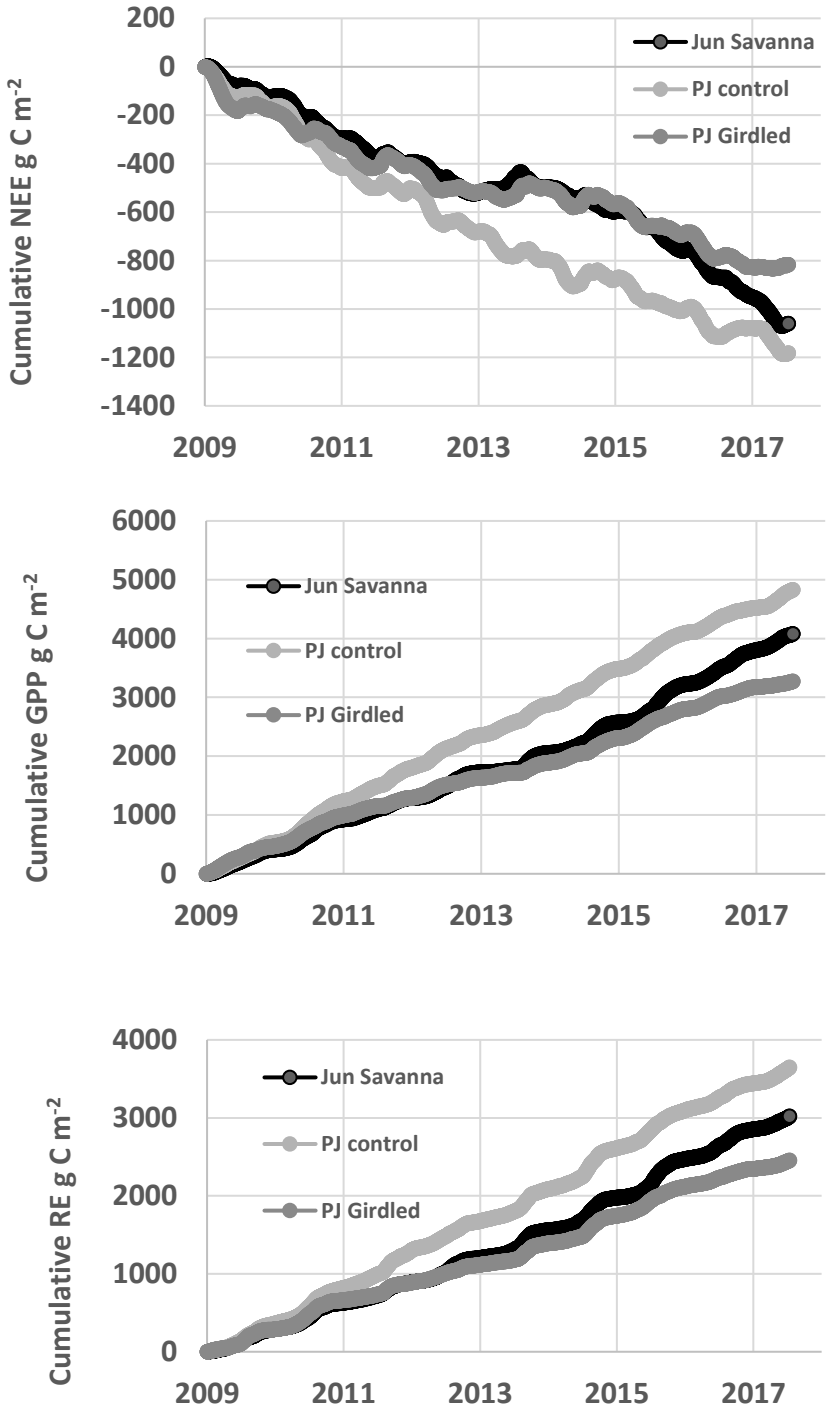

Figure 5. Cumulative NEP, GPP, Re, at PJ control, PJ Girdle and Juniper savanna from 2009-2017.

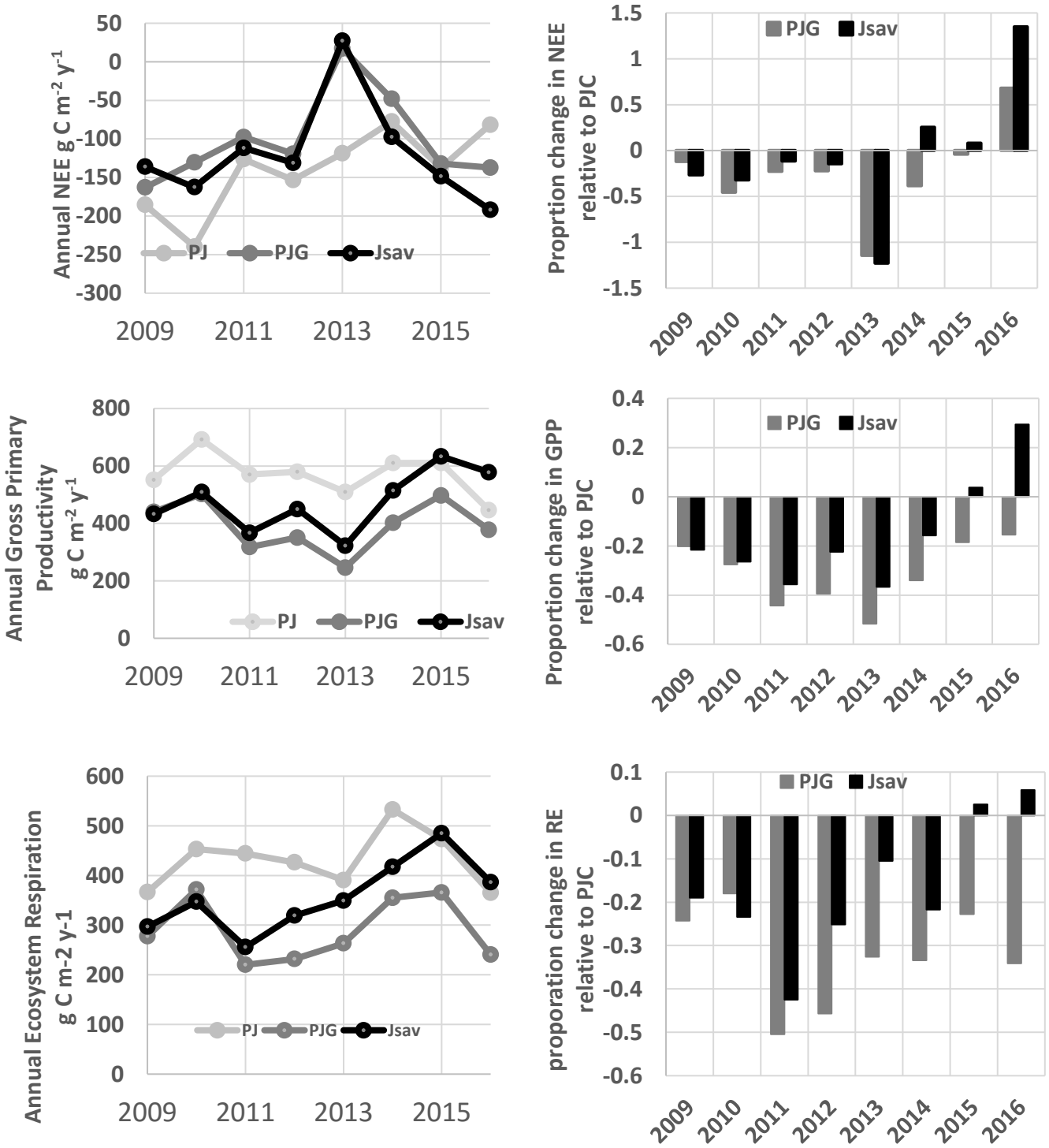

Figure 6. Annual NEP, GPP, Re, at PJ control, PJ Girdle and Juniper savanna from 2009-2016 (left column) and the proportional change in NEE, GPP and RE in PJ Girdle and Juniper savanna, compared to the PJ control site from 2009-2016.

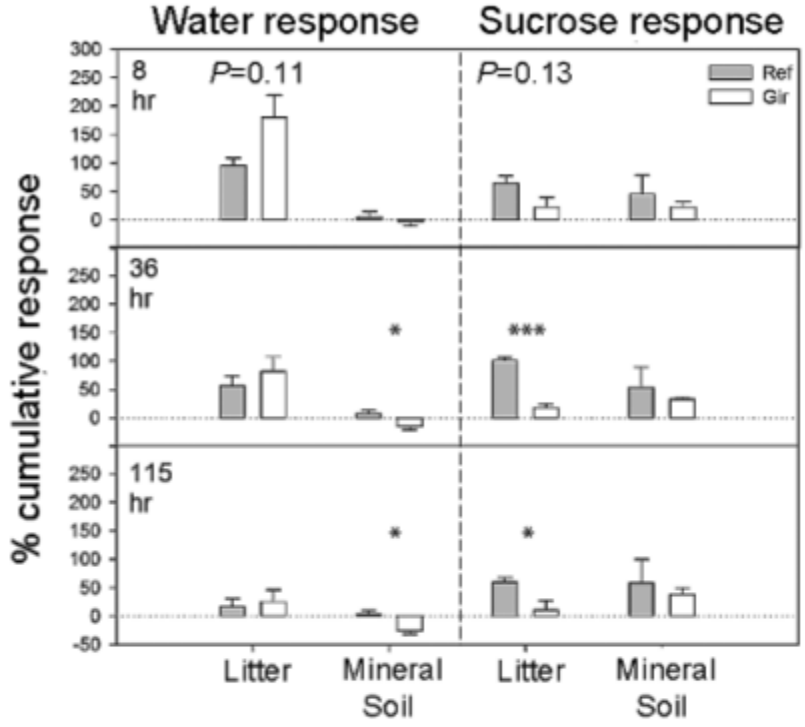

Fig. 7. Response of respiration to water and sucrose additions at the reference site (grey bars) and the girdled site (white bars). Standard error bars are shown ($n = 3$). Limitations to water and sucrose in the litter were calculated from the accumulation of respired carbon over three time periods following treatment application: from the first three measurement cycles (8 h), from the first 36 h, and from the entire duration of the experiment (115 h), using cumulative C fluxes and Eq. (1). Asterisks denote significant differences between the two sites (t-test, * $P \leq 0.05$; ** $P \leq 0.01$; *** $P \leq 0.001$). P values are shown for tests not meeting the α criteria of 0.05 but were less than 0.15.

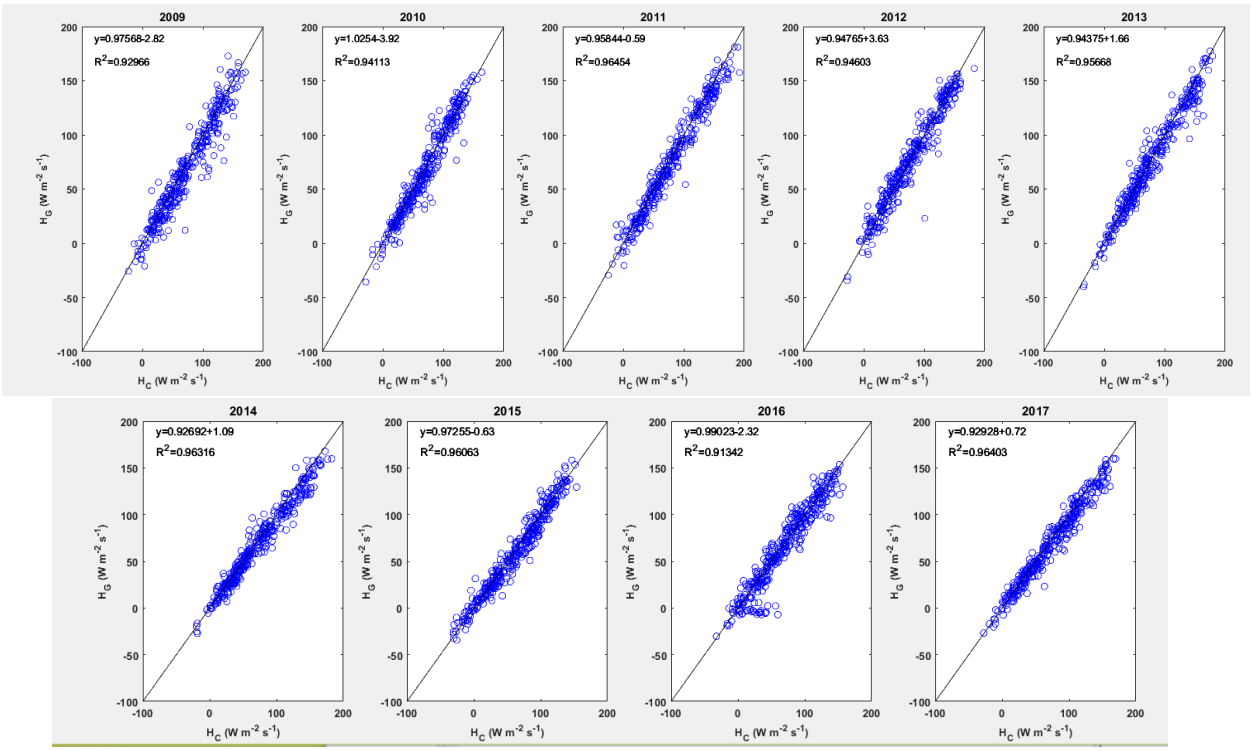

Figure 8. Comparison between sensible heat fluxes measured in girdled site (y-axis) vs. control site (x-axis from 2009-2017. Girdling or natural mortality did not significantly alter sensible heat fluxes in these PJ woodlands.

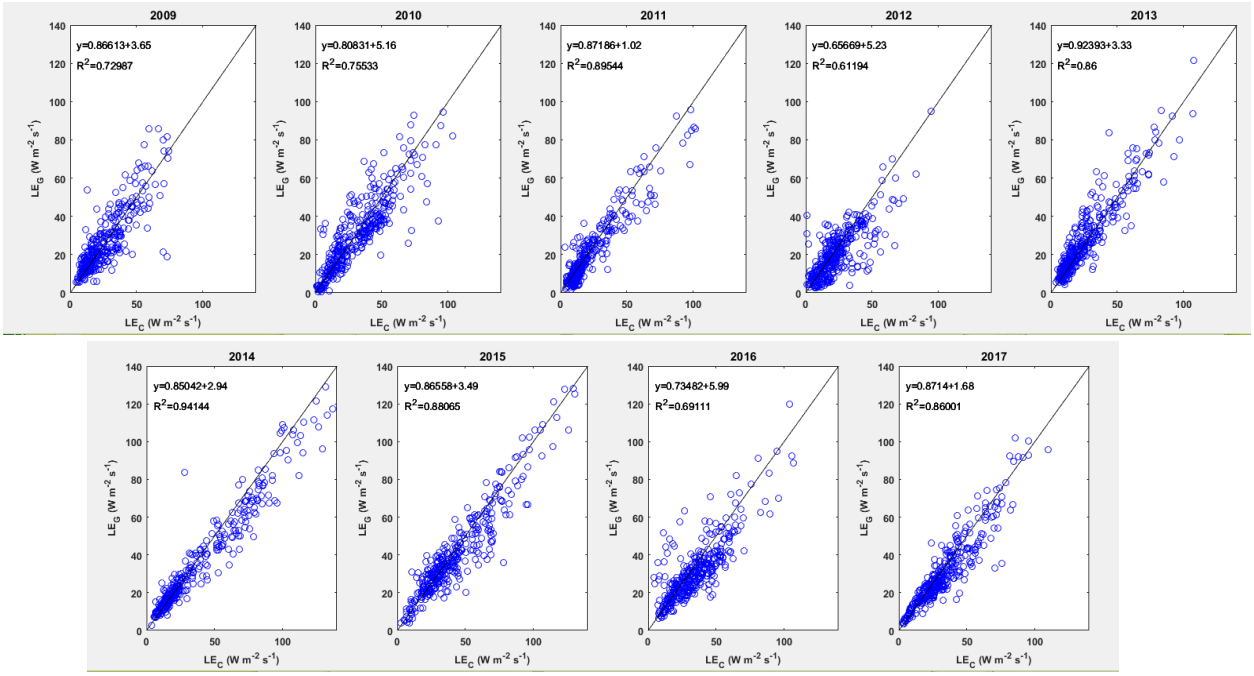

Figure 9. Comparison between latent heat fluxes measured in girdled site (y-axis) vs. control site (x-axis from 2009-2017. Girdling or natural mortality did not significantly alter latent heat fluxes in these PJ woodlands.

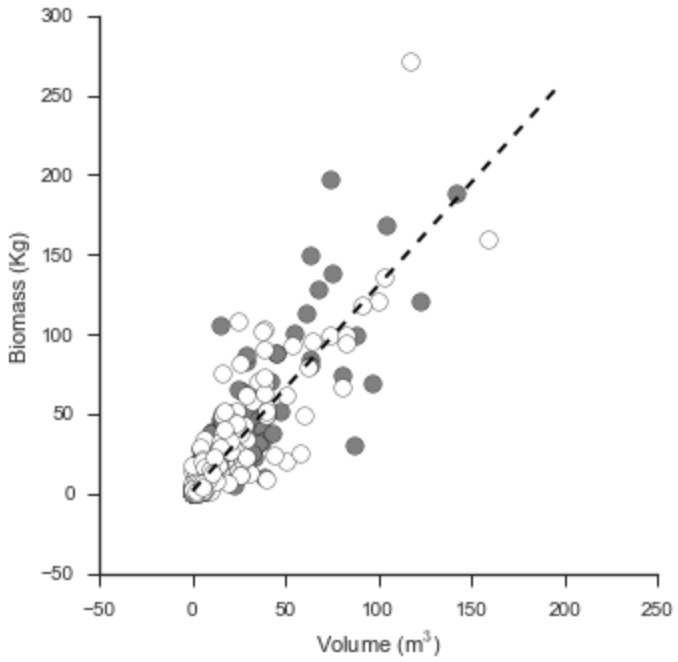

Figure 10.

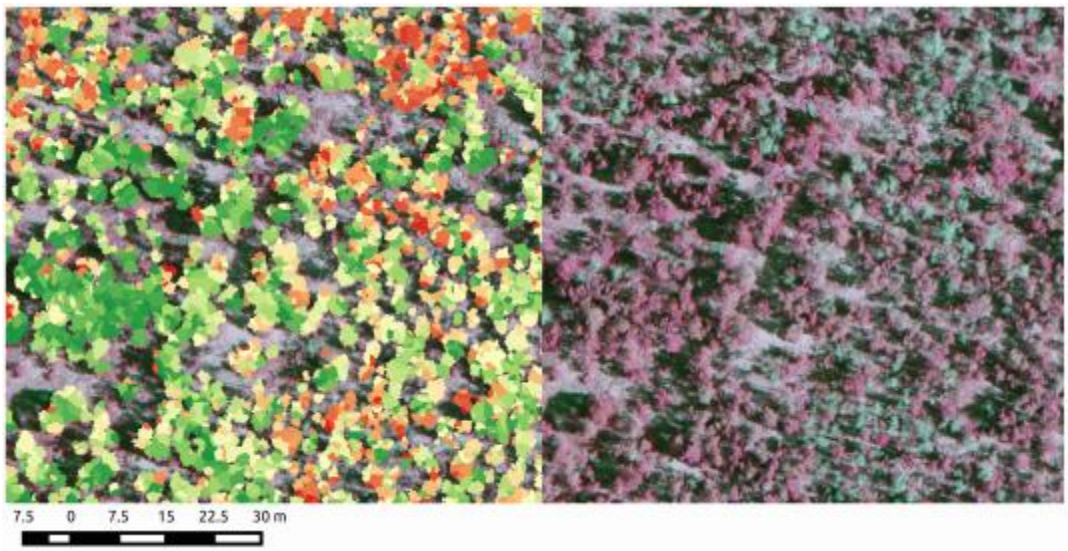

Figure 21. Camera vegetation indices and an object oriented classification, used to classify trees into live and dead groups (left) which compares well (97% accuracy) to the false-color composites of live (red) and dead (grey) vegetation in the imagery (right)

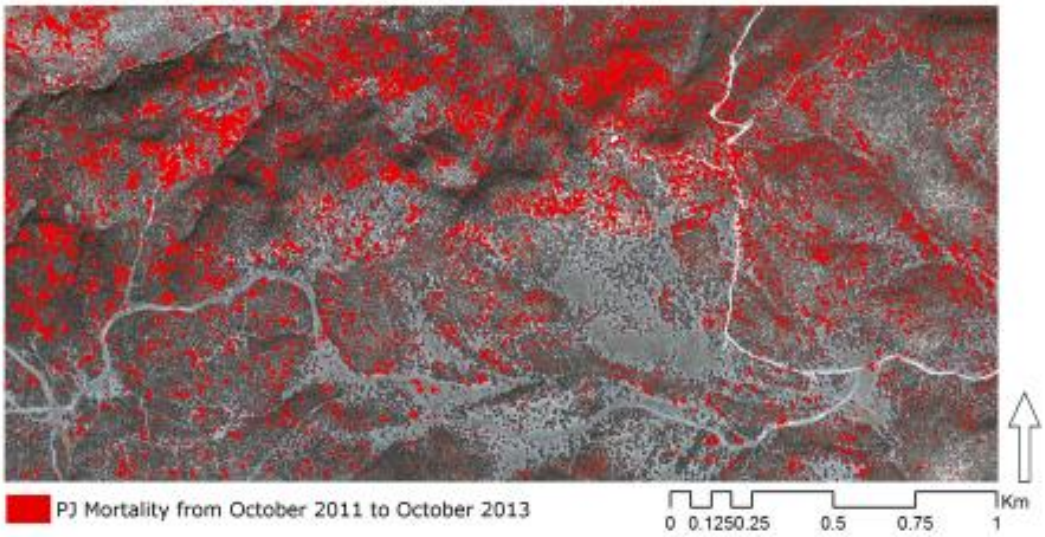

Figure 12. PJ mortality (>30%) from 2011-2013, most of it in Fall 2013 following Piñon ips outbreak derived from WorldView2 image acquisitions in 2011, 2013.

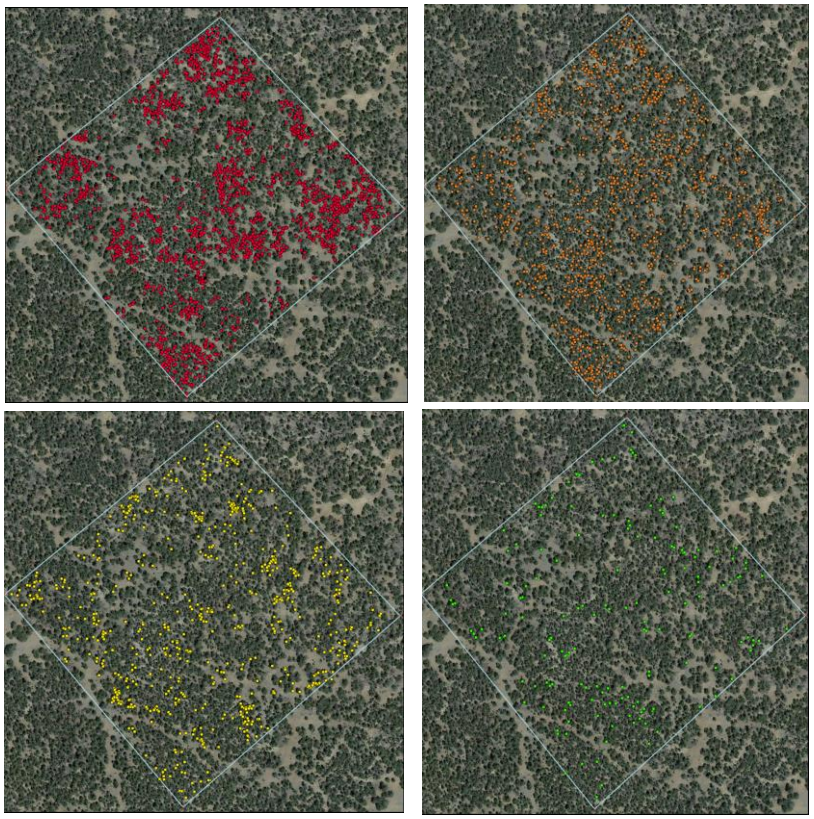

Figure 13. Progression of PJ mortality at the control site. Dots indicate dead trees as picked up by our annual mortality survey in 2014 (Top left), 2015 (top right), 2016 (bottom left), 2017 (bottom ri

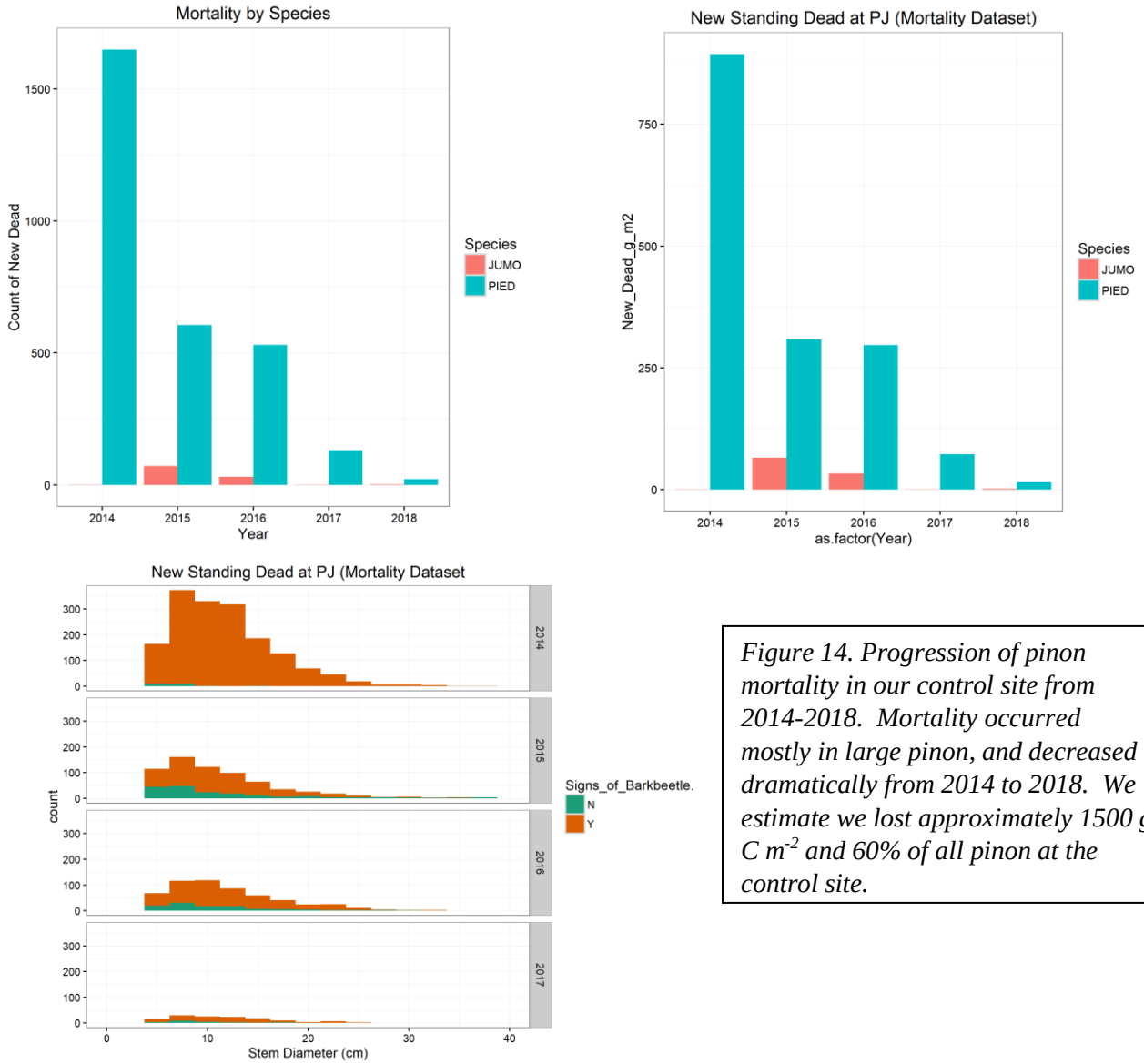

Figure 14. Progression of pinon mortality in our control site from 2014-2018. Mortality occurred mostly in large pinon, and decreased dramatically from 2014 to 2018. We estimate we lost approximately 1500 g C m^{-2} and 60% of all pinon at the control site.

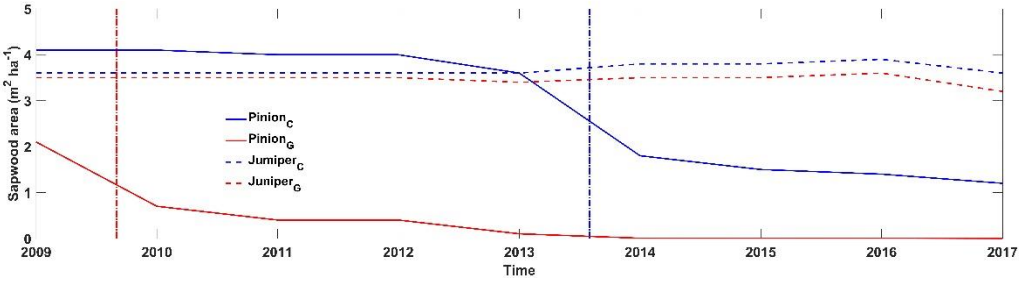

Figure 15. Change in sapwood area of both pinon and juniper in the control and girdled sites from 2009-2017.

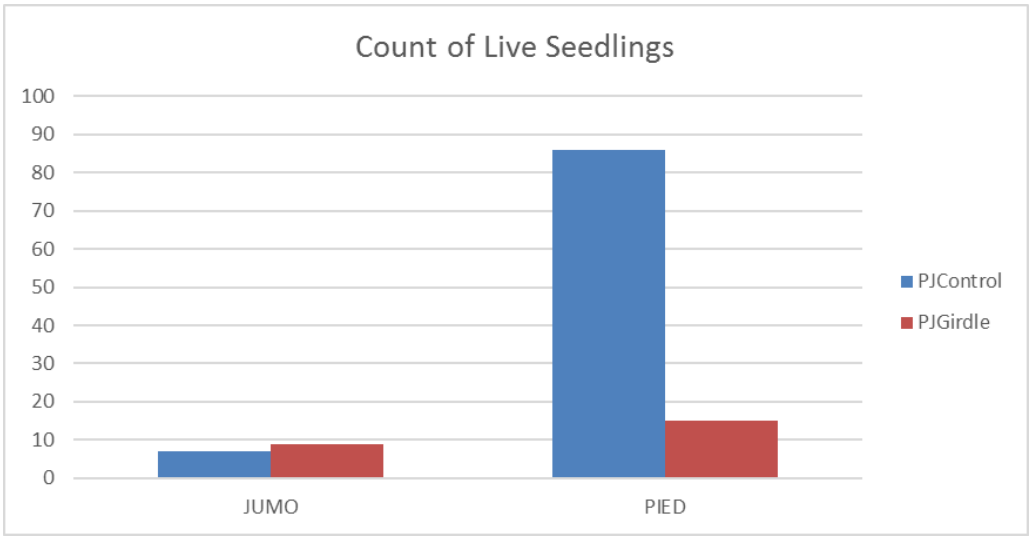

Figure 16. Change in sapwood area of both pinon and juniper in the control and girdled sites from 2009-2017.

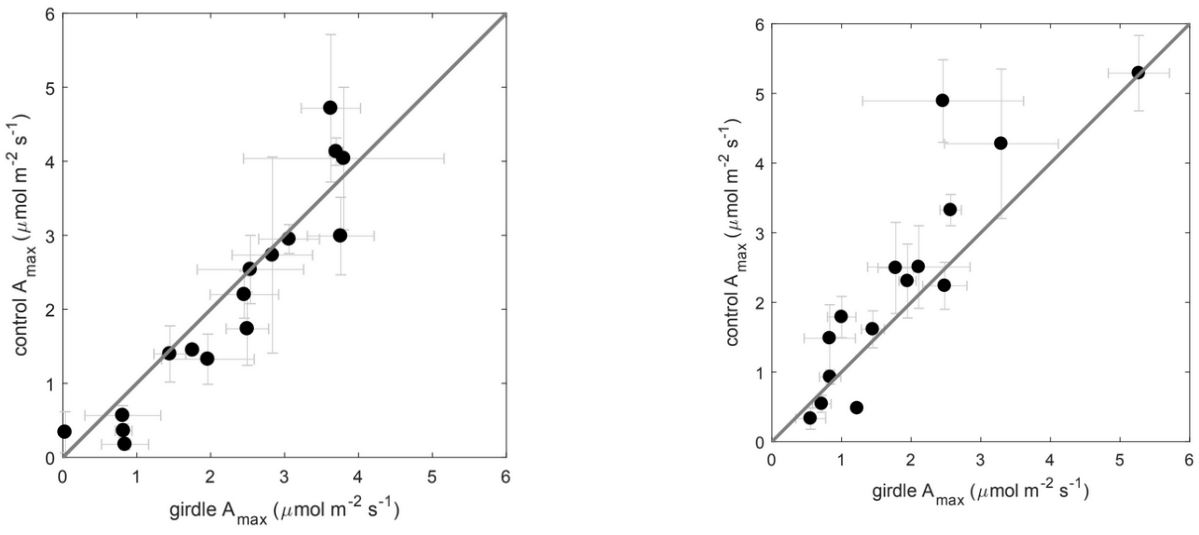

Figure 17. Amax measured in pinon trees at the control site vs. the girdled site (left), and in juniper trees measured at the control site vs. the girdled site (right). We found no significant differences between them.

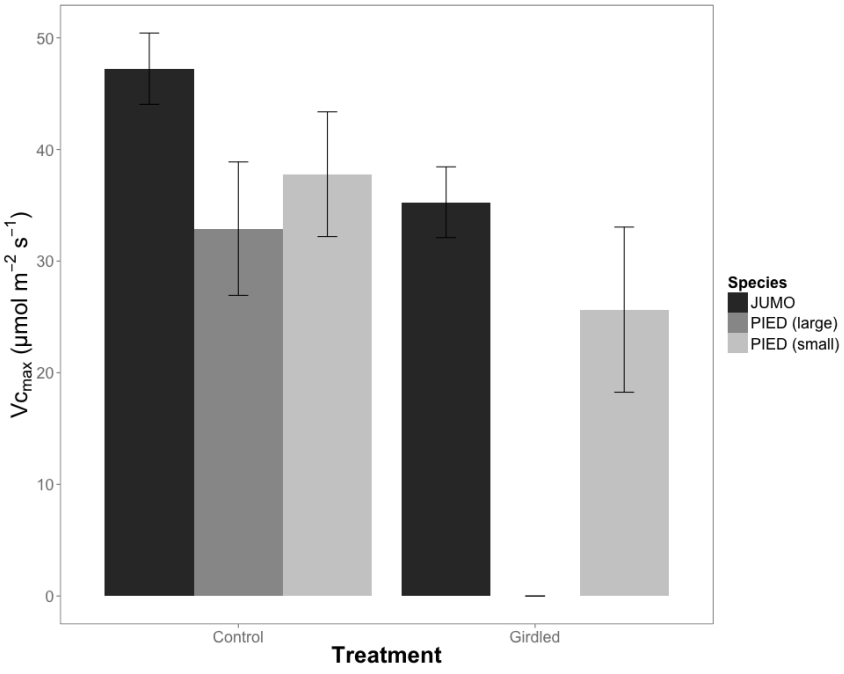

Figure 18. Vcmax measured in juniper and pinon trees in the control and girdled plots 2 years following the girdling treatment. We found no significant differences in photosynthetic capacity between the two sites.

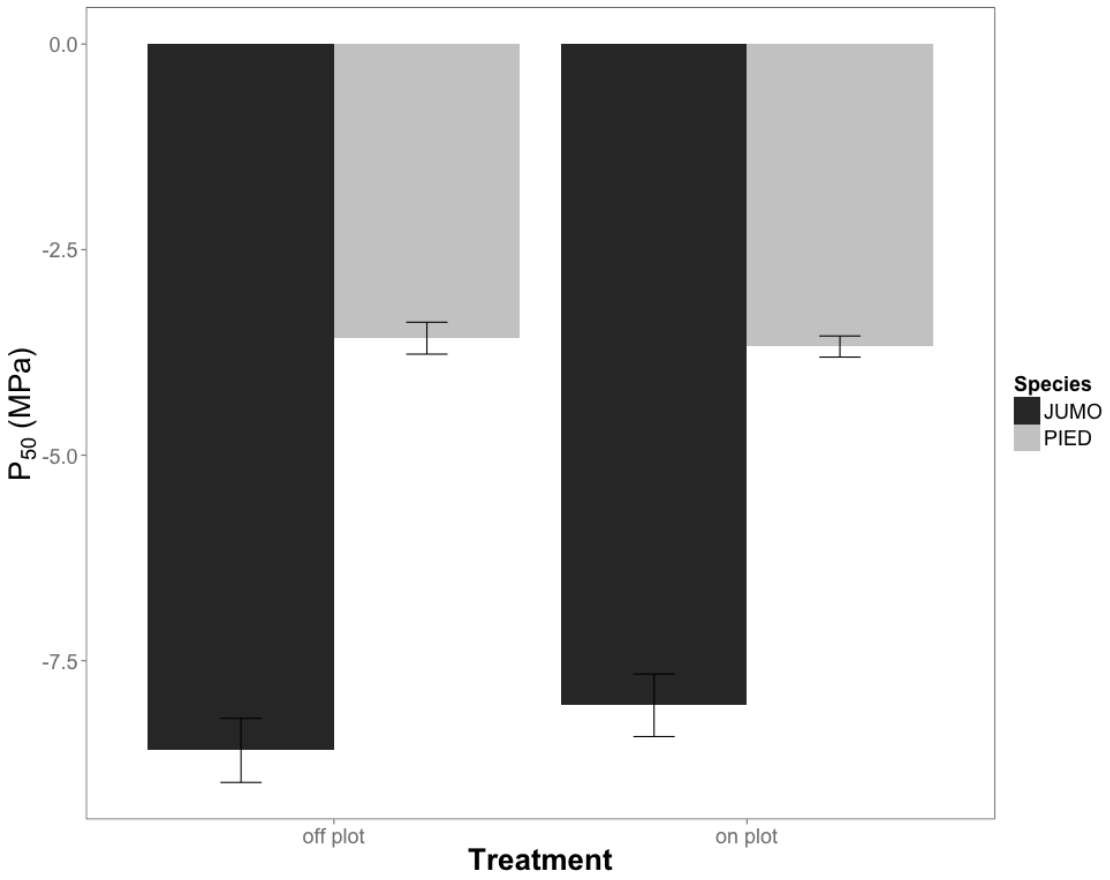

Figure 19. The water potential at which 50% of conductivity is lost (P_{50}) for juniper and piñon in the control and girdled plots. We found no significant difference in P50 between the trees in the control vs. girdled plots.

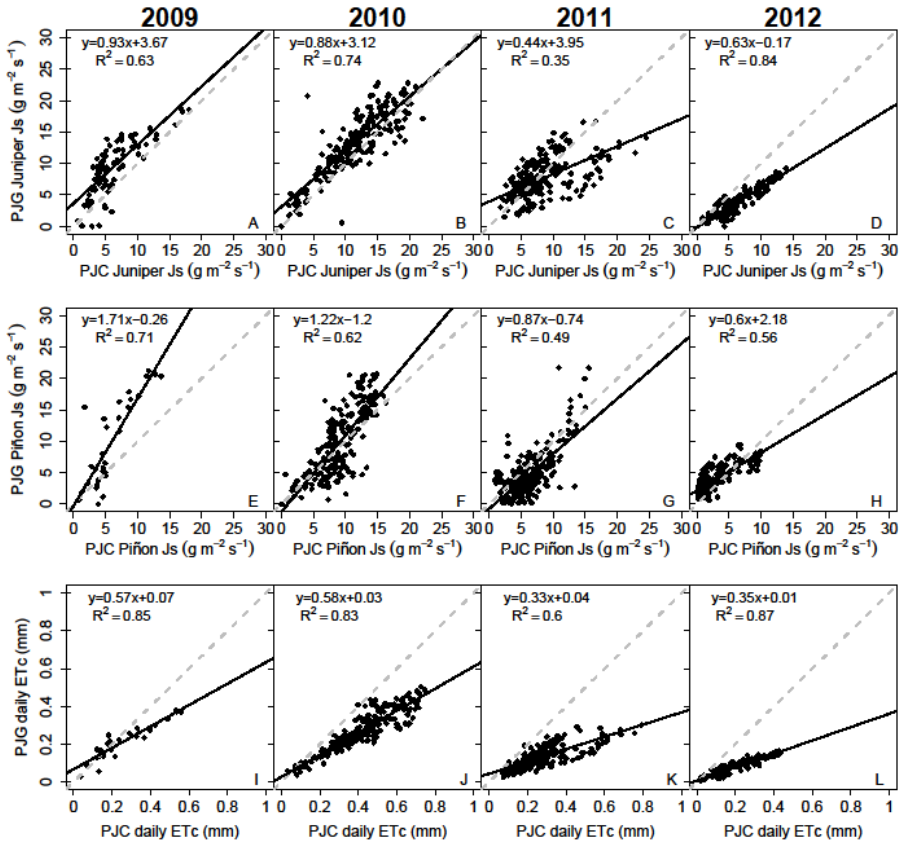

Figure 20. Comparisons between daytime mean sap flow velocity (J_s) for juniper (a-d), piñon (e-h)), and 24h totals of canopy transpiration (T_c) (i-l) at both sites (PJG on y-axis and PJC on x-axis) for each hydrological year during the study period. The grey dashed line is the 1:1 fit line, and the black solid line represents the linear fit for each regression. We only used measured (not gap-filled) J_s and T_c for this plot. R^2 is included only when correlation is significant (p-value<0.05).

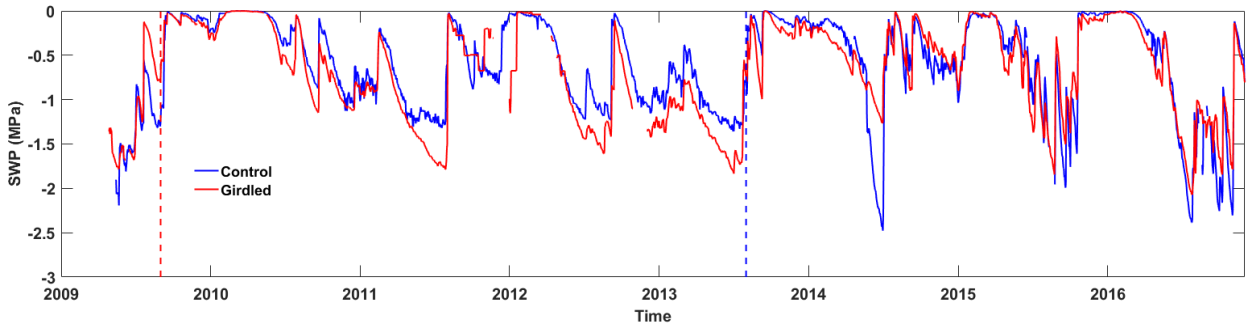

Figure 21. Overall, the girdled site became hotter and drier than the girdled site following the girdling, but this trend is starting to be reversed following the natural mortality event.

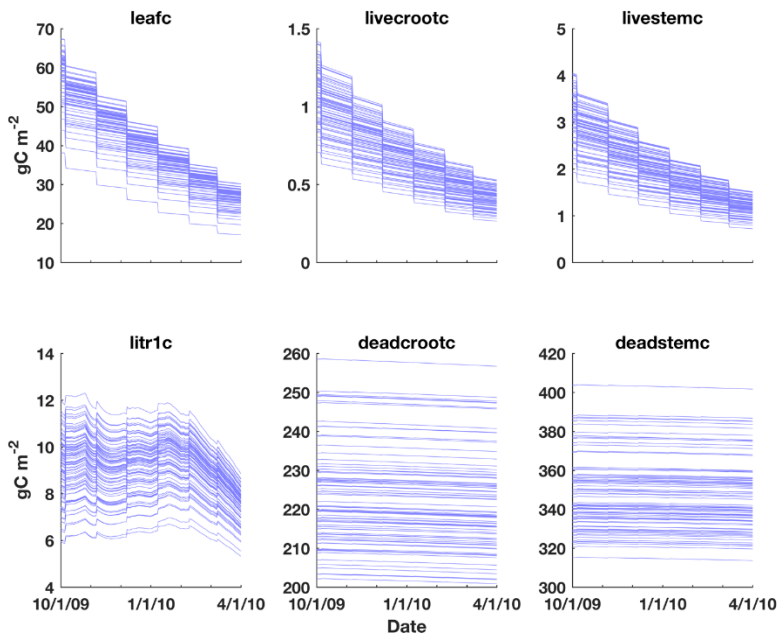

Figure 22. Examples of how live C and N pools were reduced each month (top row) and the impacts this had on the downstream litter and dead C and N pools (bottom row)

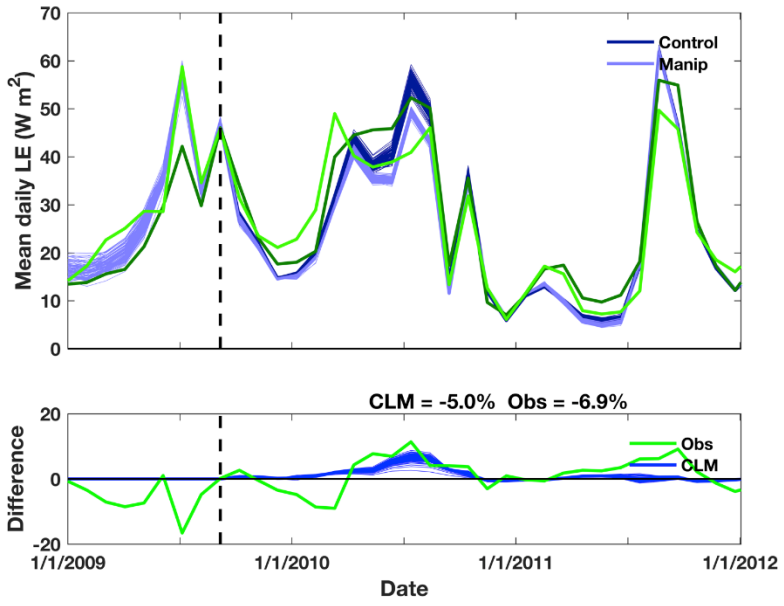

Figure 23. Observed latent heat flux at the control (dark green) and manipulation (light green) sites, and simulated latent heat fluxes.

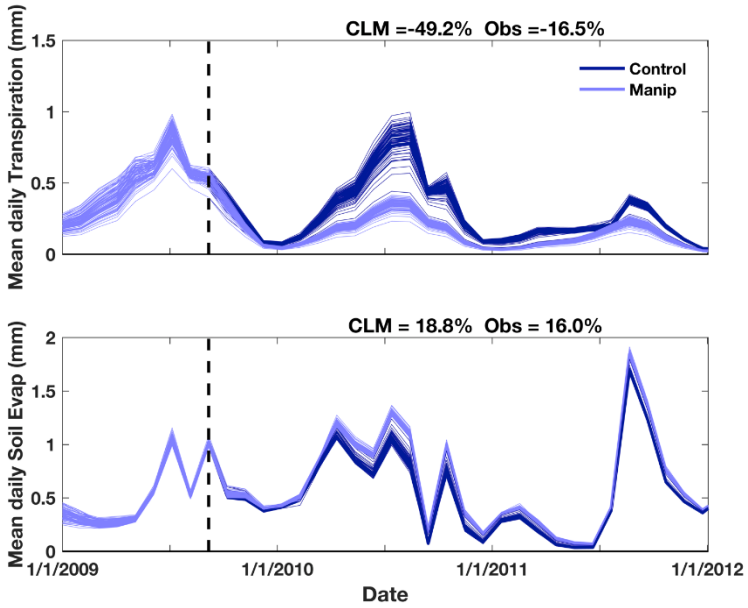

Figure 24. Modeled changes in transpiration and soil evaporation.

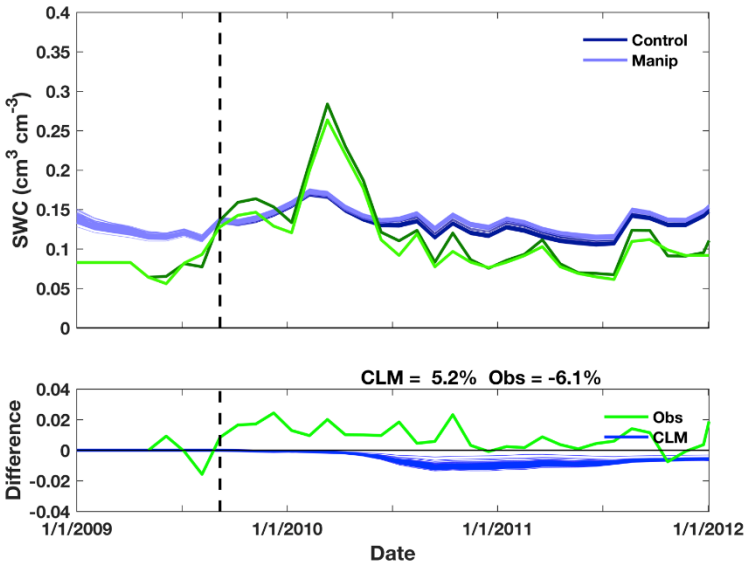

Figure 25. Observed soil moisture at the control (dark green) and manipulation (light green) sites, and the corresponding modeled values. Surprisingly, the observations indicate an increase in soil moisture, whilst the model maintains water balance.

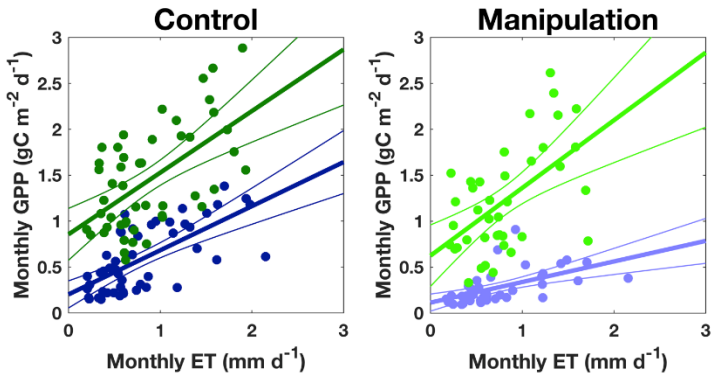

Figure 26. Ecosystem water use efficiency from flux observations (green) and modeled (blue). Whilst there is good agreement in the range of observed and model ET, the model systematically underestimates observed gross primary productivity.

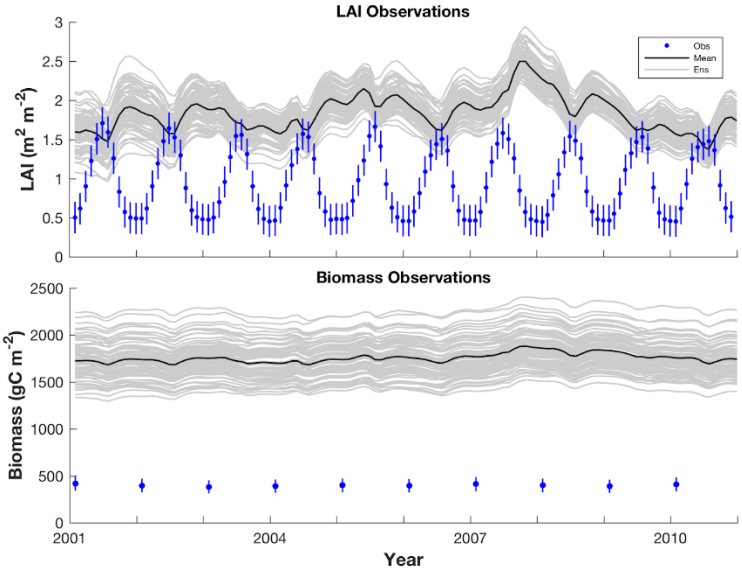

Figure 27. Time series of "observations" of LAI available at monthly time intervals, and biomass available at annual time intervals assimilated by CLM-DART.

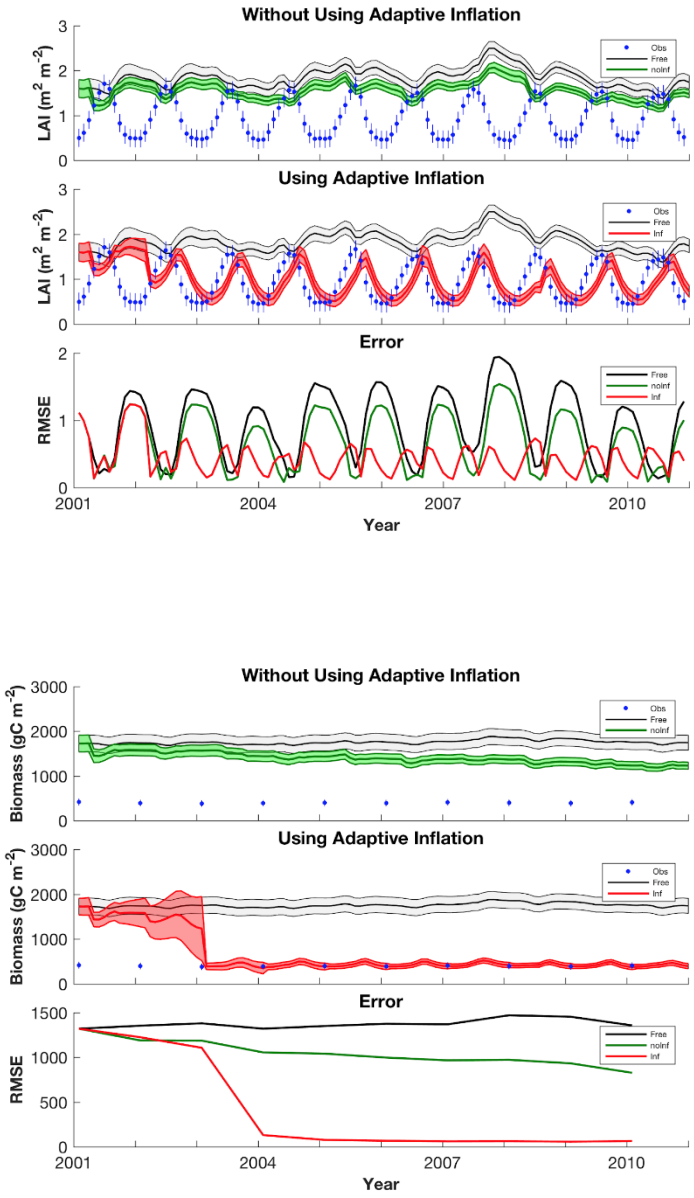

Figure 28. Forecast LAI and biomass for: (i) a free-run of the model ensemble with no assimilation; (ii) an experiment without using adaptive inflation; and (iii) using adaptive inflation, and root mean square error (RMSE) between the forecast ensemble and observations.

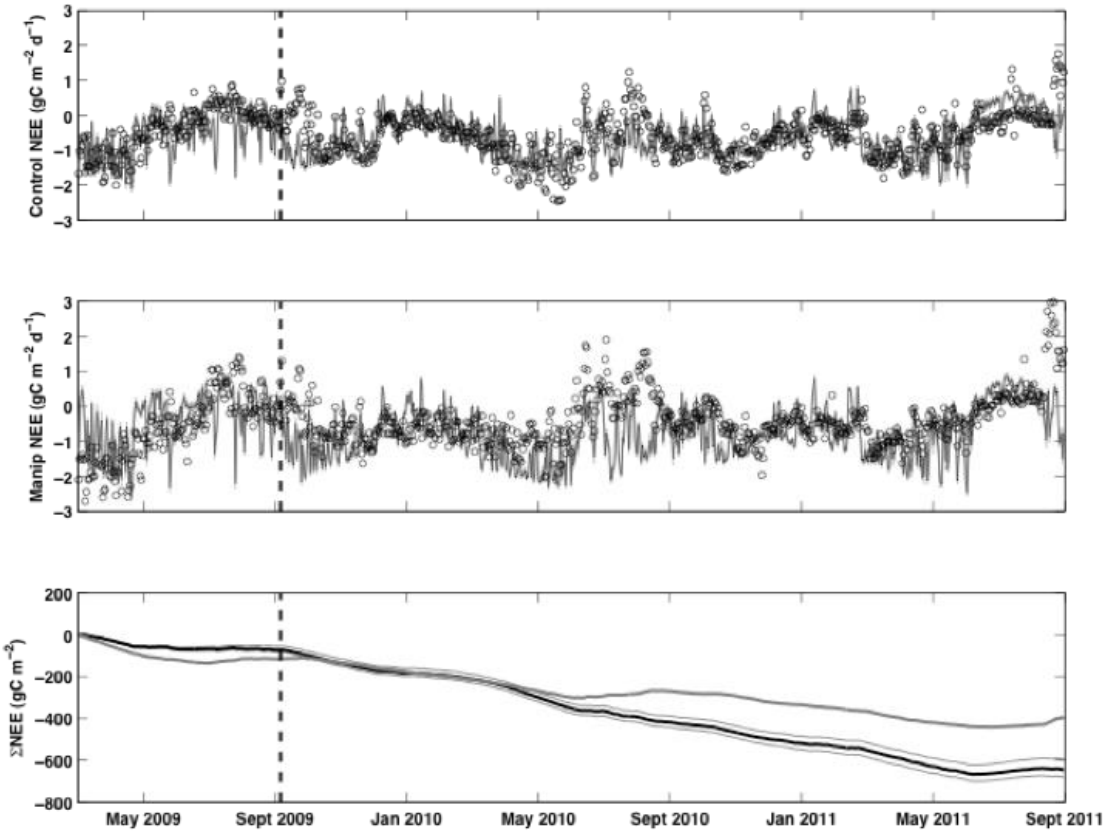

Figure 29. Daily NEE simulated with the SIPNET model at control and manipulation sites. The treatment effect is not simulated so post-treatment model and observations should not agree at the manipulation site. Confidence intervals are plotted at 95% level.

				Experiment		
			Free	*No Inf.*	*Inflation*	*Forecast*
RMSE	**LAI (m^2 m^{-2})**	*2001-2010*	0.93	0.70	0.44	-
		2006-2010	0.96	0.69	0.39	0.33
	Biomass (gC m^{-2})	*2001-2010*	1376.2	1049.9	417.7	-
		2006-2010	1406.3	940.29	62.8	51.4

Table 1. Root mean square error between model forecast ensemble LAI and biomass and LAI and biomass observations.

		Time Period					
		Pre-treatment	W1	S1	W2	S2	Post-treatment
NEE (gC m^{-2})	Control obs.	-62.3 (1.1)	-72.8 (1.1)	-143.1 (1.4)	-131.3 (1.1)	-45.9 (1.0)	-393.1 (2.6)
	Manip obs.	-89.9 (1.1)	-99.7 (1.1)	-46.9 (1.2)	-114.9 (1.0)	-5.1 (0.9)	-266.6 (2.3)
	Normalized control	*-89.9 (13.5)*	*-104.0 (13.7)*	*-195.7 (13.5)*	*-180.6 (13.7)*	*-67.6 (12.8)*	*-547.8 (30.0)*
	SIPNET control	-90.5 *(6.8)*	-109.2 *(4.2)*	-165.5 *(6.8)*	-127.0 *(5.6)*	-57.5 *(9.5)*	-459.3 *(14.1)*
	SIPNET manip	-70.3 *(7.6)*	-154.6 *(4.4)*	-200.1 *(6.4)*	-150.9 *(4.4)*	-66.2 *(9.4)*	-571.8 *(18.8)*

Table 2. Cumulative NEE for the control and manipulation sites for five six-month long time periods, and the total for two years post-treatment. The numbers in parentheses are uncertainties on these cumulative fluxes (1 standard deviation). Observations in grey shading. Normalized control uses control fluxes that have been corrected through a regression approach. SIPNET manip estimates net carbon uptake for given meteorology and initial conditions at that site as if there was no treatment and is therefore comparable to Normalized control.